



Novel carbon-based separation membranes composed of integrated zero- and one-dimensional nanomaterials

Journal:	<i>Journal of Materials Chemistry A</i>
Manuscript ID	TA-COM-11-2019-012847.R1
Article Type:	Communication
Date Submitted by the Author:	27-Dec-2019
Complete List of Authors:	Zhou, Fanglei; Rensselaer Polytechnic Institute, Tien, Huynh Ngoc; University of South Carolina DONG, QIAOBEI; Rensselaer Polytechnic Institute, Xu, Weiwei; Rensselaer Polytechnic Institute Department of Chemistry and Chemical Biology, Department of Chemistry and Chemical Biology Sengupta, Bratin; Rensselaer Polytechnic Institute Zha, Shangwen; Rensselaer Polytechnic Institute, Chemical and Biological Engineering Jiang, Ji; Rensselaer Polytechnic Institute Behera, Dinesh; Rensselaer Polytechnic Institute Department of Chemistry and Chemical Biology, Li, Shiguang; Gas Technology Institute Yu, Miao; Rensselaer Polytechnic Institute, Chemical and Biological Engineering

COMMUNICATION

Novel carbon-based separation membranes composed of integrated zero- and one-dimensional nanomaterials

Received 00th January 20xx,
Accepted 00th January 20xx

Fanglei Zhou^a, Huynh Ngoc Tien^b, Qiaobei Dong^a, Weiwei L. Xu^a, Bratin Sengupta^a, Shangwen Zha^a, Ji Jiang^a, Dinesh Behera^a, Shiguang Li^c, and Miao Yu^{a*}

DOI: 10.1039/x0xx00000x

Separation membrane structure in a large extent is determined by the membrane building block materials. To explore a new membrane structure, novel materials, including zero- (0D) and one-dimensional (1D) carbon-based materials, were studied in this work as the basic building blocks to fabricate ultrathin, compact separation membranes. Due to the intrinsic difficulty in assembling 0D graphene oxide quantum dots (GOQD) on porous substrates with much larger pores than the size of GOQD and thus low transport resistance, for the first time we report a smart strategy of depositing 1D single-walled carbon nanotube (SWCNT) as ultrathin (50 nm) "skeleton" layer to facilitate the assembly/"growth" of 0D nitrogen doped GOQDs to form densely packed 0D/1D carbon based membrane. This strategy allows evaluation of this new membrane structure composed of 0D and 1D materials as a new membrane configuration for separation applications. The 0D/1D carbon-based membranes were prepared on both hollow fiber and flat sheet substrates (pore size ≥ 25 nm) and characterized to understand the membrane structure, morphology and chemical composition. Carbon capture as a gas separation example and dye removal and desalination as water treatment examples were evaluated to demonstrate the separation potential of 0D/1D composite carbon membranes. This new membrane structure, along with the facile strategy to form ultrathin, compact coatings, may significantly expand the separation membrane technology field.

Membrane technology stands out as a highly energy-efficient separation process, compared to conventional evaporation and distillation processes which require phase transition.¹ Membrane structure, however, may affect and determine the

molecular transport path which would strongly limit the membrane permeation rate and separation efficiency.² State-of-the-art polymeric membrane matrix with micrometer thickness have been dominating the membrane separation field since the discovery of their superior separation and purification abilities in 1970s.³ Trade-off effect, nevertheless, strongly constrains polymeric membrane performance between permeability and selectivity, which could be summarized as the well-known "upper bound".⁴ Unique and unprecedented membrane structures assembled from novel membrane materials are intensely desired to overcome the upper bound of polymeric membranes. In recent decade, one-, two- and three-dimensional materials, such as carbon nanotubes,^{5, 6} graphene derivatives,⁷⁻¹³ MoS₂,¹⁴ MXene,^{15, 16} zeolites,^{17, 18} and metal organic frameworks¹⁹ were extensively explored as promising membrane building blocks for the next generation separation membranes.

So far, zero-dimensional (0D) materials have never been employed as building blocks to form new membrane structures, probably because of the challenge on depositing a few nanometer 0D materials on porous substrates. Here, we report the combination of 0D and 1D carbon-based materials to build an integrated novel membrane structure. Graphene-based quantum dots and carbon nanotubes were selected as the representative 0D and 1D materials for membrane preparation in this work. Zhang et al.²⁰ and Bacon et al.²¹ reviewed the synthesis methods of graphene quantum dots and their potential applications in energy and environment related fields, including photovoltaics,^{22, 23} organic light emitting diodes,^{24, 25} fuel cells,²⁶ catalysis,²⁷ and bioimaging and biosensing.²⁸⁻³⁰ As a derivative of graphene quantum dot, graphene oxide quantum dot (GOQD) also represents one type of the new generation 0D quantum dots material with unique properties for potential applications in many fields.³¹⁻³⁵ Moreover, doping GOQDs with heteroatoms, such as nitrogen, offers alternative strategies of effectively tuning the intrinsic properties for designing new structures and discovering new potential for various applications.^{26, 33, 36-39} To our best knowledge, however, no

^a Department of Chemical & Biological Engineering, Rensselaer Polytechnic Institute, Troy, NY 12180, United States. E-mail: yum5@rpi.edu

^b Department of Chemical Engineering and Catalysis for Renewable Fuels Center, University of South Carolina, Columbia, SC 29208, United States.

^c Gas Technology Institute, 1700 S. Mount Prospect Road, Des Plaines, IL 60018, United States.

* Corresponding Author.

† Electronic Supplementary Information (ESI) available: Experimental details. See DOI: 10.1039/x0xx00000x

effort has been made to fabricate membranes, especially ultrathin membranes, composed of 0D materials, such as N-doped GOQDs (N-GOQDs), for separation applications.

In this work, we reported a generic and facile strategy to fabricate ultrathin, compact membranes composed of 0D and 1D carbon materials on porous substrates; specifically, 0D/1D carbon-based separation membranes on porous substrates having a pore size of 20 to 30 nm were prepared for demonstration of its gas separation and water purification performance. The 0D N-GOQDs were synthesized by the carbonization of citric acid with the presence of ammonia through hydrothermal treatment (Figure S1), which is a facile and economic GOQD synthesis method.⁴⁰ The detailed preparation procedure was presented in Supplementary Information (SI). Figure 1 (a) shows a photo of the dark-yellow N-GOQD powder after drying. Figure 1 (b) are photos of N-GOQDs in DI water (0.6 mg/mL) at just prepared state (left) and after one month (right), respectively. The well-dispersed, stable N-GOQDs in water suggest their super hydrophilic feature. The UV-vis and photoluminescence spectra of N-GOQDs are presented and discussed in Figures S2-3. The as-synthesized N-GOQDs were further characterized to determine their size and composition. The TEM image of N-GOQDs in Figure 1 (c) shows that N-GOQDs are around 3 to 8 nm. The lattice fringes of a N-GOQD with a d -spacing of 0.215 nm (Figure 1 (d)) indicate a good agreement with the (100) facet of graphene and its crystalline structure.^{41, 42} The corresponding fast Fourier transform (FFT) pattern (Figure 1 (e)) exhibits the hexagonal carbon network of N-GOQDs.

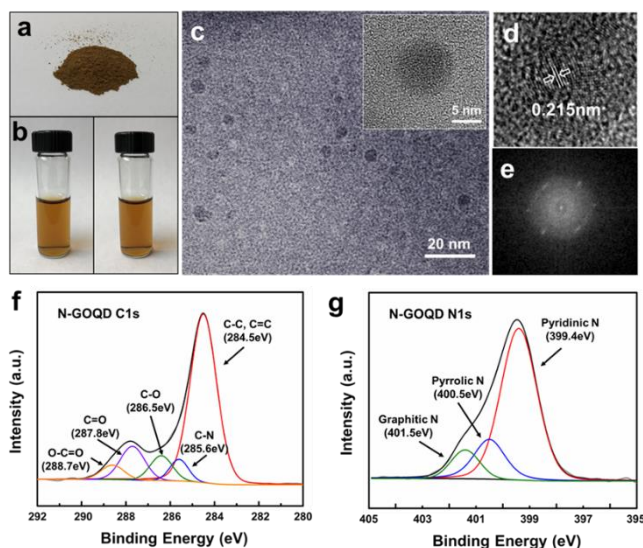


Figure 1. Characterization of N-GOQDs. Digital photos of (a) N-GOQD powder and (b) N-GOQDs dispersed in DI water at just prepared state (left) and after a month (right), respectively. (c) High-resolution TEM image of N-GOQDs; inset is the image at higher resolution. (d) TEM image showing the d_1 spacing (0.215 nm) between the lattice fringes. (e) Fast Fourier transform (FFT) pattern of N-GOQD. Deconvoluted XPS spectra of (f) C1s and (g) N1s of N-GOQDs.

X-ray photoelectron spectroscopy (XPS) full survey of N-GOQDs (Figure S4) presents a predominant graphitic C 1s peak at

around 285 eV, N 1s peak at 400 eV and O 1s peak at 532 eV. The O/C atomic ratio for as-synthesized N-GOQDs is 0.316, similar to that in others' work.^{22, 26} The N peak confirms the incorporation of N atoms into GOQDs by the hydrothermal reaction, and the N/C ratio reaches 0.139, higher than that in reported nitrogen-doped graphene quantum dots,²⁶ demonstrating the improved N atom conjugation by our synthesis method. Figure 1 (f) shows the deconvoluted C 1s spectrum of the N-GOQDs ranging from 280 to 292 eV. Five characteristic peaks emerge at 284.5, 285.6, 286.5, 287.8, and 288.7 eV, attributing to C-C, C-N, C-O, C=O, and O-C=O bonds, respectively. The high-resolution N 1s spectrum is deconvoluted in Figure 1 (g), indicating the presence of the pyridinic (399.4 eV), pyrrolic (400.5 eV), and graphitic (401.5 eV) nitrogen atoms, respectively. The high percentages of pyridinic and pyrrolic nitrogen suggest that most of the N atoms were located at the graphene panel edge.³³ Further X-ray diffraction pattern and Fourier transform infrared spectrum of N-GOQDs are illustrated in Figures S5 and S6 with more detailed analysis.

It is very challenging to deposit an ultrathin, compact coating layer composed of small 0D N-GOQDs (3-8 nm) on porous polymeric substrates with much larger pores to ensure low transport resistance. In this work, we used 30 nm-pore poly ether sulfone (PES) hollow fibers and 25 nm-pore poly sulfone (PSf) flat sheet substrate as supports. A smart and generic strategy (Figure 2(a)) for fabricating ultrathin, compact membranes composed of 0D materials was proposed in this work. An ultrathin 1D carbon based "skeleton" layer with pores smaller than or comparable to 0D materials is firstly deposited; then, the 0D materials, such as N-GOQDs, are infiltrated into the 1D nanomaterial "skeleton" as "flesh", followed by a heat treatment to form a dense layer. To maintain the similar carbon base to N-GOQDs, one-dimensional carbon material, single-walled carbon nanotube (SWCNT), was selected in this work as the 1D mesh material of the ultrathin "skeleton" layer to ensure good compatibility and low transport resistance.⁴³

SWCNT has been extensively investigated for membrane preparation in either free-standing membranes or as inorganic fillers for mixed matrix membranes due to its porous structure and prominent mechanical properties.⁴⁴ As the supporting layer, SWCNT membrane was also used for ultrathin polyamide membrane preparation.⁴³ In the current work, the 1D SWCNTs were pretreated by polydopamine (PD) to endow a hydrophilic property and thus acquire a stable dispersion in water (Supporting Note 9). Vacuum-assisted coating process was conducted to deposit an ultrathin PD wrapped SWCNT coating with several tens of nanometer thickness and a net-like structure as the carbon skeleton. As shown in Figure 2(b), the SWCNT support layer exhibits a highly interconnected net-like structure with high surface porosity, and the effective pore size is reduced to a few nanometers. In association with the highly improved hydrophilicity of the coating surface, the 1D SWCNT support layer could promise the compact 0D N-GOQD filling deposition afterwards.

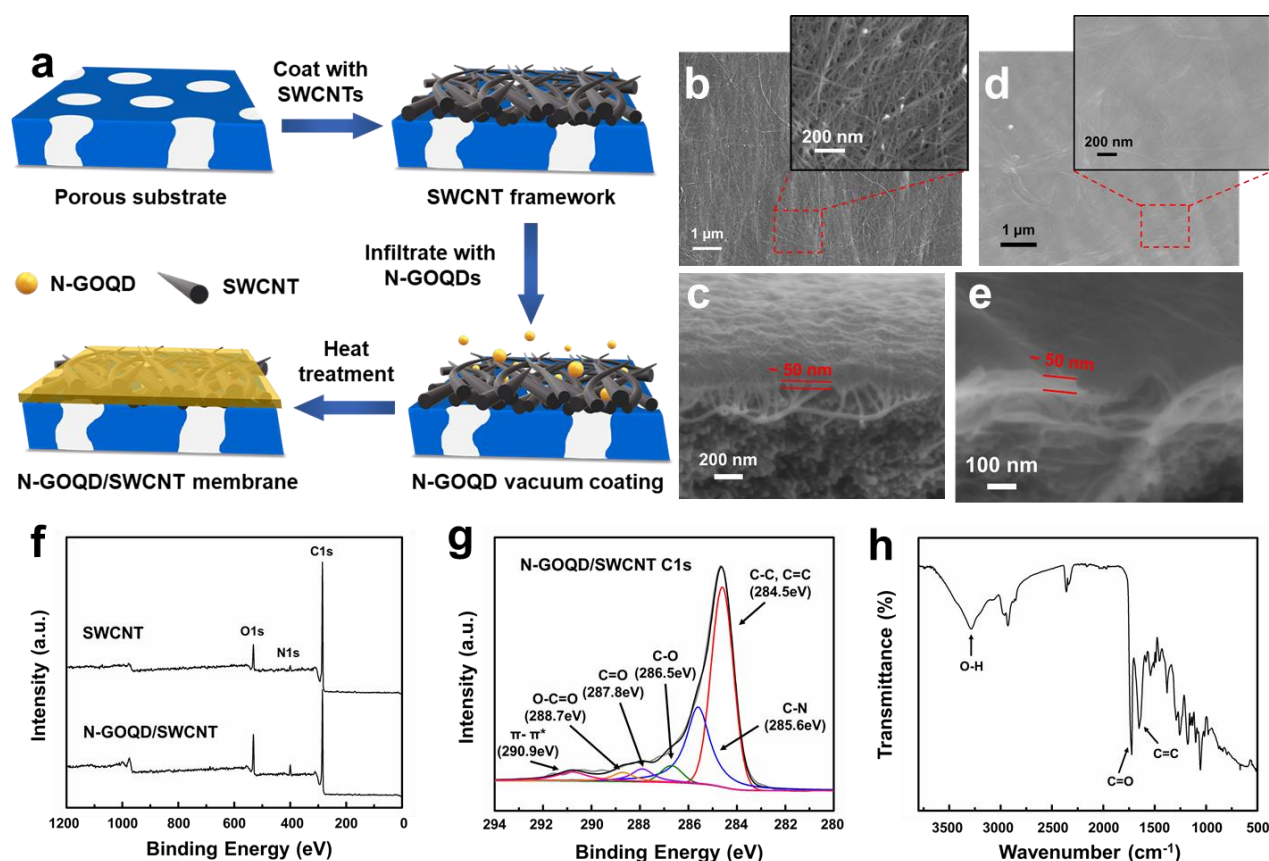


Figure 2. (a) Schematic illustration of N-GOQD/SWCNT membrane preparation. (b) Surface and (c) cross-sectional SEM images of SWCNT framework layer. (d) Surface and (e) cross-sectional SEM images of N-GOQD/SWCNT membrane. (f) XPS full surveys of SWCNT mesh and N-GOQD/SWCNT membrane. (g) Deconvoluted C1s XPS spectrum of N-GOQD/SWCNT membrane. (h) ATR-FTIR spectrum of N-GOQD/SWCNT membrane.

A proper thickness of 1D SWCNT “skeleton” layer is critical to ensure low resistance for molecular transport while facilitating assembly/“growth” of sub-10 nm size N-GOQDs between SWCNTs. We vacuum-filtrated SWCNT layer with two different thicknesses. The cross-sectional SEM images in Figure 2 (c) and Figure S7 show the thickness of SWCNT layers are 50 and 85 nm, respectively. Chemical composition characterizations for SWCNT framework are shown in Figures S8-9 and Table S1, and the XPS (Figure S8) and FTIR (Figure S9) suggested the successful coating of SWCNT layer and its carbon skeleton property with PD wrapping.

N-GOQDs were then infiltrated into the SWCNT ultrathin mesh layer by vacuum-assisted deposition, followed by a heat treatment at 80 °C for 2 h to crosslink N-GOQDs with PD wrapped SWCNTs and thus obtain the compact OD/1D (N-GOQD/SWCNT) composite membrane. The SWCNT supported N-GOQD membranes were characterized by field emission scanning electron microscopy (FESEM). The membrane surface morphology is shown in Figure 2 (d); a uniform, dense and high-quality membrane layer was formed by completely filling SWCNT mesh pores with N-GOQDs. The SWCNT backbone under the coating layer can still be seen, demonstrating that the membrane structure consists of carbon skeleton and carbon quantum dots filling units. The ultrathin thickness is revealed by

the cross-sectional SEM image (Figure 2 (e)), which shows an approximately 50 nm thick membrane layer on the polymer support. The chemical composition of the as-prepared N-GOQD/SWCNT membrane was examined by XPS and FTIR spectroscopy. Figure 2 (f) shows the elemental surveys of 1D SWCNT framework and N-GOQD/SWCNT composite membrane, respectively. After incorporating SWCNT framework with N-GOQDs, the oxygen and nitrogen content increased from 7.0 and 2.7% to 14.5 and 6.5%, respectively, suggesting the successful loading of N-GOQDs in the SWCNT skeleton. The deconvoluted C1s spectrum (Figure 2 (g)) clearly exhibits C=O and O-C=O peaks, resulting from the carboxyl groups at the edge of N-GOQDs. Compared to the C1s spectrum of N-GOQDs (Figure 1 (f)) and SWCNT mesh (Figure S8), the slightly enhanced C-N peak could be an evidence of the crosslinking between the N-GOQDs and the PD coating on SWCNTs. The FTIR spectrum (Figure 2 (h)) further verified the N-GOQD/SWCNT membrane chemical composition. As compared to the SWCNT skeleton (Figure S9), new peaks at 1,651 and 1,753 cm⁻¹ emerged because of the C=C and C=O stretching vibrations from N-GOQD carbon panel and carboxyl groups. The peak at 3,297 cm⁻¹ corresponds to the -OH groups on the surface of N-GOQDs. The contact angle (CA) measurement was conducted for SWCNT mesh and N-GOQD/SWCNT membrane, respectively, as shown in Figure S10. The SWCNT support shows only slight CA decrease

as compared to the polymer substrate. The N-GOQD/SWCNT membrane, however, exhibits significantly hydrophilic surface after the infiltration of N-GOQDs.

To explore the separation potential of the novel 0D/1D N-GOQD/SWCNT composite membrane, water treatment and CO₂ capture from flue gas were both investigated in this work as application examples of liquid filtration and gas separation, respectively. For water treatment, we investigated the nanofiltration and desalination performance of this quantum dot membrane. The N-GOQD/SWCNT membrane was fabricated on PSf flat-sheet ultrafiltration membranes (Figure S11) via two-step vacuum assisted coating as shown in Figure S12. Different dye molecules with negative charge (methyl orange (MO) and rose bengal (RB)) and positive charge (methylene blue (MB) and crystal violet (CV)) and Na₂SO₄ were dissolved in water and studied as filtration objects. The molecular weight, charge and size of different dyes were listed in Table S2. The N-GOQD/SWCNT membrane surface is expected to exhibit negative charge due to the carboxyl groups around the quantum dot edge.

The procedure of filtration tests was presented in SI and the membrane sample was shown in Figure S13. The water permeability and rejection of the base PSf substrate were shown in Table S3, and our membrane filtration results were shown in Figure 3. For the 1D SWCNT “skeleton”, it shows moderate/low water treatment performance in terms of the low rejection of smaller dyes and divalent salt. According to the zeta potential measurement in Figure S14, the membrane surface is negatively charged, therefore for negatively charged dyes, charge effect could increase the rejection as an additional factor to pore size exclusion; for positively charged dyes, the pore size exclusion would dominate the rejection performance due to the minimized charge effect. As a result, the negatively charged SWCNT membrane rejected 84.5% RB, but only 16.4% MO with smaller molecular size. In strong contrast, the N-GOQD/SWCNT membrane showed significantly higher rejection for MO (87.2%) with a water permeance of 11.31 (±0.89) L/(m²·h·bar) (LMH/bar) and almost 100% rejection for RB. The N-GOQD/SWCNT membrane exhibited 75.4% and 86.6% rejection for MB and CV, respectively, which are predominantly higher than 1D SWCNT framework membrane. The desalination

performance was investigated with divalent salt on both SWCNT “skeleton” and N-GOQD/SWCNT membranes. 47.0% rejection with a water permeance of 8.95 LMH/bar was observed for N-GOQD/SWCNT membrane, whereas SWCNT mesh layer only exhibited 3.6% rejection. The rejection of large dye molecules is apparently attributed to the size exclusion from those interstices between the N-GOQDs. These dye rejection and salt removal results demonstrate the great potential of the N-GOQD/SWCNT membrane for water purification applications.

The CO₂ capture performance was then studied to demonstrate the gas separation potential of N-GOQD/SWCNT membrane. To ensure a high packing density for future practical use, the membrane was fabricated on PES hollow fiber substrate with 30 nm pores on the inner surface (Figure S15). The detailed N-GOQD/SWCNT hollow fiber membrane preparation procedure was presented in SI. Figures S16-18 show the lab-designed hollow fiber membrane module and coating system, similar to our previous work.^{7, 9} A digital photo of the coated N-GOQD/SWCNT hollow fiber membrane is shown in Figure S19. Compared to PES blank substrate, a uniform gray color on the inner surface of hollow fiber was observed, suggesting a high-quality coating.

The gas permeation measurements were conducted with our lab-designed permeation system (Figures S20-21) on 1D SWCNT “skeleton” layer and 0D/1D N-GOQD/SWCNT composite membranes with mixed gas (15% CO₂/85% N₂) to explore their transport resistance and base selectivity. Consequently, the N-GOQD/SWCNT membrane showed a CO₂/N₂ selectivity of 29 with CO₂ permeance of 96 GPU and the detailed result was presented in SI (Supporting Note 20). The gas molecular transport in the hydrated N-GOQD/SWCNT membrane can be explained by the well-known solution-diffusion mechanism.^{45, 46} Similar to glassy and rubbery polymer membranes, the hydrated N-GOQD/SWCNT membrane can be presented as a “poly-0D quantum dot” matrix, and the free volume, which is the Angstrom-sized interstices, is expected to be formed between the nano-meter sized zero-dimensional quantum dots and carbon nanotube skeleton. Gas molecules would dissolve into the hydrated “poly-0D quantum dot” matrix and then diffuse to the low chemical potential side as shown in the inset diagram of Figure 4 (a).

Based on the low CO₂ separation performance of N-GOQD/SWCNT membranes as discussed in SI and our previous studies^{7, 9} on GO-amine hollow fiber membranes for CO₂ capture, N-GOQD/SWCNT membrane transport interstices can be functionalized by crosslinking CO₂-philic agents, such as amine molecules, to highly boost gas permeance and selectivity. Targeting carbon capture in this work, amines could be good additives to facilitate CO₂ transport and potentially crosslink with the as-produced N-GOQD membrane. We have successfully functionalized our GO hollow fiber membranes by adding piperazine and ethylenediamine in our previous work and the highly-efficient CO₂ capture performance was observed.^{7, 9} Here, we pre-functionalized our 0D N-GOQDs with

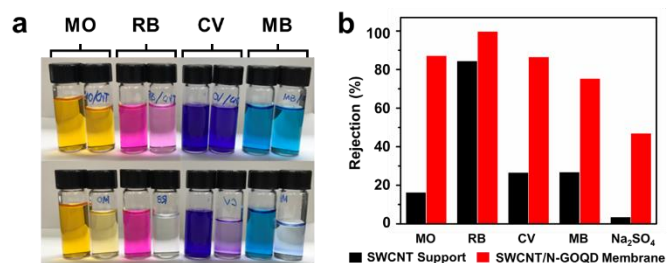


Figure 3. Nanofiltration and desalination performance of SWCNT/N-GOQD membrane. (a) Photo of dye solutions before and after rejection tests by SWCNT support layer (top row) and N-GOQD/SWCNT membrane (bottom row), respectively. For each dye, left is the feed solution and right is the permeate solution. (b) Rejection of nanofiltration and desalination measurements.

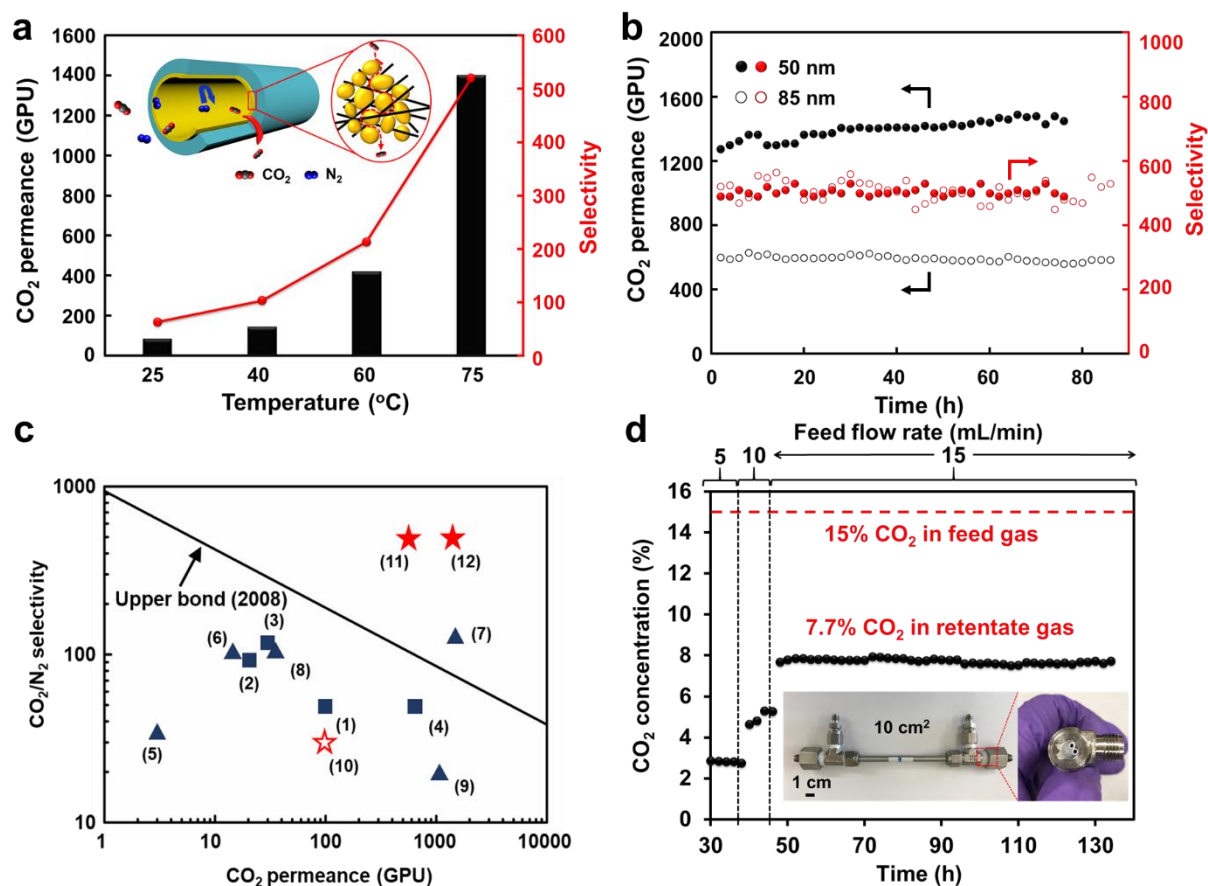


Figure 4. CO₂ separation performance of DETA functionalized N-GOQD/SWCNT hollow fiber membranes. (a) Temperature effect on membrane (50 nm thickness) separation performance. The inserted figure shows the CO₂ molecular transport path in the N-GOQD/SWCNT matrix. (b) Long-term run of DETA functionalized N-GOQD/SWCNT hollow fiber membranes with two different thicknesses (85 nm and 50 nm). (c) Membrane performance comparison on 2008 Robeson upper bond plot. (1) GO,⁵¹ (2) GO-Pebax,⁵² (3) GO-PEI-Pebax,⁵³ (4) GO-Borate,⁵⁴ (5) Pebax-PEG-POSS,⁵⁵ (6) PEI-Silica-Pebax,⁵⁶ (7) PDMS,⁵⁷ (8) PVAm,⁵⁸ (9) PEG-based,⁵⁹ (10) Base N-GOQD/SWCNT hollow fiber membrane in this work. (11) and (12) DETA functionalized N-GOQD/SWCNT hollow fiber membrane with 85 and 50 nm thickness, respectively, in this work. (d) Long-term run of 10 cm² DETA functionalized N-GOQD/SWCNT hollow fiber membrane (50 nm thickness). The retentate CO₂ concentration was monitored and the flow rate was adjusted from 5, 10 to 15 mL(STP)/min on the feed side.

another amine, diethylenetriamine (DETA), which has three amine functionalities and thus is expected to have very high capacity for binding CO₂ and high absorption rate.⁴⁷⁻⁴⁹ The detailed functionalization was demonstrated in SI (Supporting Note 21), and the functionalized material was characterized by XPS (Figure S22). With the same coating method for N-GOQD/SWCNT membranes, the DETA functionalized N-GOQD hollow fiber membrane was prepared on the 1D SWCNT “skeleton” layer with two different thicknesses (50 and 85 nm).

In addition to the facilitated transport of CO₂ offered by the amine functionalization on N-GOQD/SWCNT membrane,^{7, 9} DETA could also possibly act as a crosslinker to bond OD N-GOQD material with 1D SWCNT mesh, and thus fortify the carbon-based composite membrane structure. As shown in the surface SEM image (Figure S23), the backbone of SWCNT mesh can still be seen, while all the pores and gaps have been fully filled with DETA functionalized N-GOQDs. With a further heat treatment, amine groups on DETA could react with the functional groups at the surface of PD wrapped SWCNTs and

crosslink more N-GOQDs on SWCNTs to form a rigid carbon matrix structure. The carbon-based membrane layer possesses enormous oxygen and amine functional groups, which significantly favor CO₂ and water transport. The cross-sectional SEM image (Figure S23)) of one membrane prepared on 50-nm SWCNT mesh shows that the effective membrane thickness is still around 50 nm, indicating the ultrathin selective separation layer which promises the high gas permeance. The XPS spectrum of DETA functionalized N-GOQD/SWCNT membrane is shown in Figure S24. The nitrogen peak intensity increased significantly, owing to the incorporated amine molecules in the transport interstices. The ATR-FTIR spectrum (Figure S25) further verified the amine functionalization, as N-H stretching and bending vibrations at 2,851, 2,917, and 1,580 cm⁻¹, and C-N stretching at 1,245 cm⁻¹ were clearly observed.

The gas permeation result of DETA functionalized N-GOQD/SWCNT membrane at room temperature was discussed in SI (Supporting Note 22) where a low separation performance was found. We then increased the permeation temperature and

found the CO₂ permeance increased exponentially with the increase of temperature, and reached CO₂ permeance of ~1,450 GPU and CO₂/N₂ selectivity of ~520 at 75 °C (Figure 4 (a)). Instead of solution-diffusion mechanism, the facilitated transport mechanism dominates the CO₂ molecular transport process across the DETA functionalized N-GOQD/SWCNT membrane layer. The bonded amine molecules act as CO₂ carriers to reversibly react with CO₂ molecules at the high concentration side (feed side) and generate bicarbonate molecules, which could rapidly transport in the membrane interstices and dissociate to CO₂ again at the low concentration side (permeate side).^{7, 9, 50} The feed absolute pressure was increased from 114 kPa to 161 kPa, and the CO₂ permeance decreased gradually as the pressure increases as shown in Figure S26, further demonstrating the facilitated transport mechanism which favors more for the low pressure permeation process. The high activation energy for CO₂ permeation in DETA functionalized N-GOQD/SWCNT membrane (48.42 kJ/mol as shown in Figure S27) suggests activated diffusion of CO₂ in the membrane due to the chemical bonding.

Long-term stability of DETA functionalized N-GOQD/SWCNT membrane was examined for two membranes with different membrane thicknesses as shown in Figure 4 (b). For the 85-nm membrane, the CO₂ permeance maintained at about 600 GPU with CO₂/N₂ selectivity at around 500. For the thinner N-GOQD/SWCNT membrane (50 nm), the CO₂ permeance increased to 1,450 GPU with 520 CO₂/N₂ selectivity, mainly due to the thinner selective membrane layer and thus a shorter transport pathway for gas molecules. Membrane performance was also compared with other published data⁵¹⁻⁵⁹ and Robeson upper bound (2008) in Figure 4 (c), in which the CO₂ permeability is replaced by the CO₂ permeance by assuming 100 nm thickness for polymeric membranes. Our DETA functionalized N-GOQD/SWCNT membrane shows superior performance as compared to others.

Large-area (10 and 50 cm²) N-GOQD hollow fiber membranes were also prepared with the same method to show the potential for scalability and potential for effective CO₂ capture from flue gas as shown in Figure 4 (d) and Figures S28-30. During the separation test for the 10 cm² membrane, the retentate CO₂ concentration was monitored to demonstrate the practical carbon capture efficiency. The feed gas flow rate was adjusted from 5 to 15 mL (STP)/min. At 5 and 10 mL/min feed flow rate, the retentate CO₂ concentration could be decreased to 2.8% and 5.0%, respectively. To achieve 50% CO₂ removal from the feed, 15 mL/min was determined as the maximum flow rate of the simulated flue gas for a 10 cm² DETA functionalized N-GOQD/SWCNT hollow fiber membrane. With 134-h run, membrane exhibited very stable CO₂ capture performance, and the concentration of CO₂ could be efficiently decreased from 15% in the feed gas to ~7.7% at 75 °C.

Conclusions

In summary, we successfully developed a facile and effective method to fabricate high-quality and ultrathin separation

membranes by using 0D N-GOQD and 1D SWCNT nanomaterial. The novel 0D/1D carbon-based composite membrane can be synthesized on both flat-sheet and hollow fiber substrates, and its promising separation performance on both water purification and gas permeation was demonstrated. In addition, the strategy of assembling 0D materials into 1D skeleton to form ultrathin 2D film could be extensively expanded to different 0D and 1D nanomaterials or nanoparticles possessing unique properties, and thus may be applied for other applications other than membrane separation.

Conflicts of interest

There are no conflicts to declare.

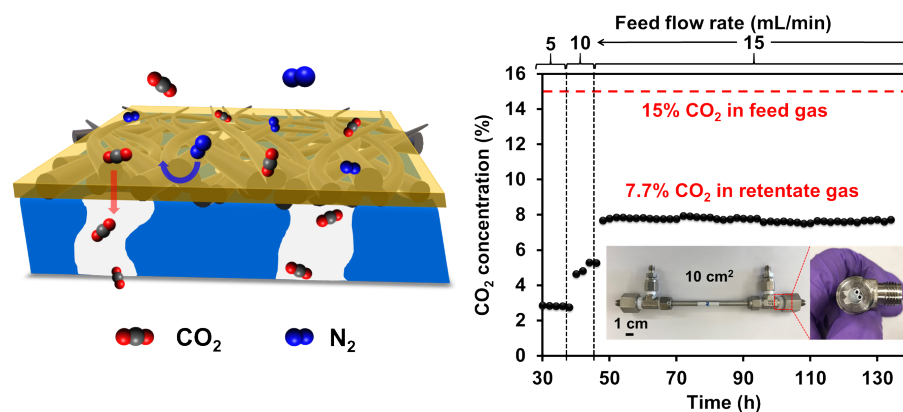
Acknowledgements

The authors thank the support by the Department of Energy (DOE) under the contract No. DE-FE0026383, and the help from the filtration measurement by Shijie Zhang, the XPS measurement by Dr. Robert Planty, the FESEM measurement by Dr. M. David Frey, and the XRD measurement by Dr. Joel Morgan.

References

- 1 P. Bernardo, E. Drioli and G. Golemme, *Ind. Eng. Chem. Res.*, 2009, **48**, 4638-4663.
- 2 W. J. Koros and C. Zhang, *Nat. Mater.*, 2017, **16**, 289.
- 3 L. M. Robeson, *J. Membr. Sci.*, 1991, **62**, 165-185.
- 4 L. M. Robeson, *J. Membr. Sci.*, 2008, **320**, 390-400.
- 5 J. K. Holt, H. G. Park, Y. Wang, M. Stadermann, A. B. Artyukhin, C. P. Grigoropoulos, A. Noy and O. Bakajin, *Science*, 2006, **312**, 1034-1037.
- 6 B. J. Hinds, N. Chopra, T. Rantell, R. Andrews, V. Gavalas and L. G. Bachas, *Science*, 2004, **303**, 62-65.
- 7 F. Zhou, H. N. Tien, W. L. Xu, J.-T. Chen, Q. Liu, E. Hicks, M. Fathizadeh, S. Li and M. Yu, *Nat. Commun.*, 2017, **8**, 2107.
- 8 M. Fathizadeh, W. L. Xu, F. Zhou, Y. Yoon and M. Yu, *Adv. Mater. Interfaces*, 2017, **4**, 1600918.
- 9 F. Zhou, H. N. Tien, Q. Dong, W. L. Xu, H. Li, S. Li and M. Yu, *J. Membr. Sci.*, 2019, **573**, 184-191.
- 10 F. Zhou, M. Fathizadeh and M. Yu, *Annu. Rev. Chem. Biomol.*, 2018, **9**, 17-39.
- 11 W. L. Xu, F. Zhou and M. Yu, *Ind. Eng. Chem. Res.*, 2018, **57**, 16103-16109.
- 12 W. L. Xu, C. Fang, F. Zhou, Z. Song, Q. Liu, R. Qiao and M. Yu, *Nano Lett.*, 2017, **17**, 2928-2933.
- 13 M. Fathizadeh, W. L. Xu, M. Shen, E. Jeng, F. Zhou, Q. Dong, D. Behera, Z. Song, L. Wang and A. Shakouri, *Environ. Sci.: Water Res. Technol.*, 2019.
- 14 L. Sun, H. Huang and X. Peng, *Chem. Commun.*, 2013, **49**, 10718-10720.
- 15 L. Ding, Y. Wei, Y. Wang, H. Chen, J. Caro and H. Wang, *Angew. Chem. Int. Ed.*, 2017, **56**, 1825-1829.
- 16 L. Ding, Y. Wei, L. Li, T. Zhang, H. Wang, J. Xue, L.-X. Ding, S. Wang, J. Caro and Y. Gogotsi, *Nat. Commun.*, 2018, **9**, 155.
- 17 Z. Song, Q. Dong, W. L. Xu, F. Zhou, X. Liang and M. Yu, *ACS Appl. Mater. Interfaces*, 2017, **10**, 769-775.
- 18 Q. Dong, Z. Song, F. Zhou, H. Li and M. Yu, *Micropor. Mesopor. Mat.*, 2019, **281**, 9-14.
- 19 J.-R. Li, R. J. Kuppler and H.-C. Zhou, *Chem. Soc. Rev.*, 2009, **38**, 1477-1504.
- 20 Z. Zhang, J. Zhang, N. Chen and L. Qu, *Energy Environ. Sci.*, 2012, **5**, 8869-8890.

- 21 M. Bacon, S. J. Bradley and T. Nann, *Part. Part. Syst. Char*, 2014, **31**, 415-428.
- 22 Y. Li, Y. Hu, Y. Zhao, G. Shi, L. Deng, Y. Hou and L. Qu, *Adv. Mater*, 2011, **23**, 776-780.
- 23 X. Yan, X. Cui, B. Li and L.-s. Li, *Nano Lett*, 2010, **10**, 1869-1873.
- 24 V. Gupta, N. Chaudhary, R. Srivastava, G. D. Sharma, R. Bhardwaj and S. Chand, *J. Am. Chem. Soc*, 2011, **133**, 9960-9963.
- 25 D. I. Son, B. W. Kwon, D. H. Park, W.-S. Seo, Y. Yi, B. Angadi, C.-L. Lee and W. K. Choi, *Nat. Nanotechnol*, 2012, **7**, 465.
- 26 Y. Li, Y. Zhao, H. Cheng, Y. Hu, G. Shi, L. Dai and L. Qu, *J. Am. Chem. Soc*, 2011, **134**, 15-18.
- 27 S. Zhuo, M. Shao and S.-T. Lee, *ACS Nano*, 2012, **6**, 1059-1064.
- 28 S. Zhu, J. Zhang, S. Tang, C. Qiao, L. Wang, H. Wang, X. Liu, B. Li, Y. Li, W. Yu, X. Wang, H. Sun and B. Yang, *Adv. Funct. Mater*, 2012, **22**, 4732-4740.
- 29 M. Zhang, L. Bai, W. Shang, W. Xie, H. Ma, Y. Fu, D. Fang, H. Sun, L. Fan and M. Han, *J. Mater. Chem*, 2012, **22**, 7461-7467.
- 30 S. Zhu, J. Zhang, C. Qiao, S. Tang, Y. Li, W. Yuan, B. Li, L. Tian, F. Liu and R. Hu, *Chem. Commun*, 2011, **47**, 6858-6860.
- 31 F. Zhang, F. Liu, C. Wang, X. Xin, J. Liu, S. Guo and J. Zhang, *ACS Appl. Mater. Interfaces*, 2016, **8**, 2104-2110.
- 32 F. Liu, M.-H. Jang, H. D. Ha, J.-H. Kim, Y.-H. Cho and T. S. Seo, *Adv. Mater*, 2013, **25**, 3657-3662.
- 33 T. F. Yeh, C. Y. Teng, S. J. Chen and H. Teng, *Adv. Mater*, 2014, **26**, 3297-3303.
- 34 D. L. Zhao and T.-S. Chung, *Water Res*, 2018, **147**, 43-49.
- 35 W. Gai, D. L. Zhao and T.-S. Chung, *Water Res*, 2019, **154**, 54-61.
- 36 K. Gong, F. Du, Z. Xia, M. Durstock and L. Dai, *Science*, 2009, **323**, 760-764.
- 37 Y.-C. Lin, C.-Y. Lin and P.-W. Chiu, *Appl. Phys. Lett*, 2010, **96**, 133110.
- 38 H. Liu, Y. Liu and D. Zhu, *J. Mater. Chem*, 2011, **21**, 3335-3345.
- 39 M. Favaro, L. Ferrighi, G. Fazio, L. Colazzo, C. Di Valentin, C. Durante, F. Sedona, A. Gennaro, S. Agnoli and G. Granozzi, *ACS Catalysis*, 2015, **5**, 129-144.
- 40 M. Fathizadeh, H. N. Tien, K. Khivantsev, Z. Song, F. Zhou and M. Yu, *Desalination*, 2019, **451**, 125-132.
- 41 Q. Liu, B. Guo, Z. Rao, B. Zhang and J. R. Gong, *Nano Lett*, 2013, **13**, 2436-2441.
- 42 J. Peng, W. Gao, B. K. Gupta, Z. Liu, R. Romero-Aburto, L. Ge, L. Song, L. B. Alemany, X. Zhan and G. Gao, *Nano Lett*, 2012, **12**, 844-849.
- 43 Y. Zhu, W. Xie, S. Gao, F. Zhang, W. Zhang, Z. Liu and J. Jin, *Small*, 2016, **12**, 5034-5041.
- 44 S. Iijima, *Nature*, 1991, **354**, 56.
- 45 J. G. Wijmans and R. W. Baker, *J. Membr. Sci*, 1995, **107**, 1-21.
- 46 P. M. Budd and N. B. McKeown, *Polym. Chem*, 2010, **1**, 63-68.
- 47 K. Fu, G. Chen, T. Sema, X. Zhang, Z. Liang, R. Idem and P. Tontiwachwuthikul, *Chem. Eng. Sci*, 2013, **100**, 195-202.
- 48 A. Hartono, K. A. Hoff, T. Mejdell and H. F. Svendsen, *Energy Procedia*, 2011, **4**, 179-186.
- 49 C.-H. Yu, H.-H. Cheng and C.-S. Tan, *Int. J. Greenh. Gas Con*, 2012, **9**, 136-147.
- 50 W. J. Koros and R. Mahajan, *J. Membr. Sci*, 2000, **175**, 181-196.
- 51 H. W. Kim, H. W. Yoon, S.-M. Yoon, B. M. Yoo, B. K. Ahn, Y. H. Cho, H. J. Shin, H. Yang, U. Paik, S. Kwon, J.-Y. Choi and H. B. Park, *Science*, 2013, **342**, 91-95.
- 52 J. Shen, G. Liu, K. Huang, W. Jin, K. R. Lee and N. Xu, *Angew. Chem. Int. Ed*, 2015, **127**, 588-592.
- 53 X. Li, Y. Cheng, H. Zhang, S. Wang, Z. Jiang, R. Guo and H. Wu, *ACS Appl. Mater. Interfaces*, 2015, **7**, 5528-5537.
- 54 S. Wang, Y. Wu, N. Zhang, G. He, Q. Xin, X. Wu, H. Wu, X. Cao, M. D. Guiver and Z. Jiang, *Energy Environ. Sci*, 2016, **9**, 3107-3112.
- 55 M. M. Rahman, V. Filiz, S. Shishatskiy, C. Abetz, S. Neumann, S. Bolmer, M. M. Khan and V. Abetz, *J. Membr. Sci*, 2013, **437**, 286-297.
- 56 H. Wu, X. Li, Y. Li, S. Wang, R. Guo, Z. Jiang, C. Wu, Q. Xin and X. Lu, *J. Membr. Sci*, 2014, **465**, 78-90.
- 57 S. Li, Z. Wang, X. Yu, J. Wang and S. Wang, *Adv. Mater*, 2012, **24**, 3196-3200.
- 58 Y. Shen, H. Wang, J. Liu and Y. Zhang, *ACS Sustain. Chem. Eng*, 2015, **3**, 1819-1829.
- 59 Q. Fu, J. Kim, P. A. Gurr, J. M. Scofield, S. E. Kentish and G. G. Qiao, *Energy Environ. Sci*, 2016, **9**, 434-440.



Zero-dimensional graphene oxide quantum dots and one-dimensional carbon-nanotubes were integrated to form ultrathin membranes for CO₂ capture and water purification.